Vol. 22: 25–41, 2014
doi: 10.3354/ab00587

AQUATIC BIOLOGY
Aquat Biol

Published November 20

Contribution to the Theme Section 'Environmental forcing of aquatic primary productivity'

Effect of CO_2, nutrients and light on coastal plankton. I. Abiotic conditions and biological responses

P. J. Neale[1,*], C. Sobrino[2], M. Segovia[3], J. M. Mercado[4], P. Leon[4], M. D. Cortés[4], P. Tuite[4], A. Picazo[5], S. Salles[4], M. J. Cabrerizo[6], O. Prasil[7], V. Montecino[8], A. Reul[3], A. Fuentes-Lema[2]

[1]Smithsonian Environmental Research Center, Edgewater, Maryland 21037, USA
[2]Department of Ecology and Animal Biology, Faculty of Sciences, University of Vigo, 36310 Vigo, Spain
[3]Department of Ecology, Faculty of Sciences, University of Málaga, 29071 Málaga, Spain
[4]Centro Oceanográfico de Málaga, Instituto Español de Oceanografía, 29640 Fuengirola, Málaga, Spain
[5]Departamento de Microbiología y Ecología (Siberia II), Instituto Cavanilles de Biodiversidad y Biología Evolutiva (ICBiBE), Universidad de Valencia, 46100 Burjassot (Valencia), Spain
[6]Department of Ecology, Faculty of Sciences, University of Granada, 18071 Granada, Spain
[7]Laboratory of Photosynthesis, Center Algatech, Institute of Microbiology ASCR, 37981 Trebon, Czech Republic
[8]Departamento de Ciencias Ecológicas, Facultad de Ciencias, Universidad de Chile, Casilla 653 Santiago, Chile

ABSTRACT: We report on results of a microcosm experiment to study the interactive effects of elevated CO_2, high organic and inorganic nutrient loading, and high irradiance on phytoplankton and bacterioplankton from the Mediterranean coastal ecosystem of the Alboran Sea. This experiment was part of the Group for Aquatic Productivity 9th international workshop and was conducted by Working Group 1 (WG1: Phytoplankton of coastal waters, www.gap9.uma.es). Over a 7 d period, we measured the variation in physical and chemical variables and the characteristics of phytoplankton and bacterioplankton in microcosms incubated under 8 treatments, representing full factorial combinations of 2 levels each of CO_2 supply, nutrient concentrations and solar radiation exposure. For each treatment combination, we incubated triplicate microcosms consisting of 20 l polyethylene bags which were transparent to ultraviolet radiation. Sustained growth of phytoplankton biomass (chl *a*) occurred in all treatments. The absence of mesozooplankton in the microcosms resulted in a trophic cascade. Picophytoplankton were initially stimulated but then decreased, apparently due to microzooplankton grazing, and were largely replaced by diatoms. Bacteria were also initially stimulated and then decreased, but eventually recovered. Responses were modified markedly by nutrient enrichment and light availability, with moderate effects of elevated CO_2. Relative to ambient CO_2, elevated CO_2 resulted in higher chl *a* under low irradiance, but lower chl *a* under high irradiance.

KEY WORDS: Phytoplankton · Bacterioplankton · CO_2 · Ultraviolet radiation · Nutrients · Multiple stressors · Microcosm · Trophic cascade

INTRODUCTION

All ecosystems on Earth are now influenced by man's activities, which are changing the environment in multiple ways at an accelerating pace (Vitousek et al. 1997, Halpern et al. 2008). Widespread effects are expected to occur over the coming decades, resulting in an alteration of the planet's geological, biological, and ecological systems. In marine microbial communities, ongoing and future changes are expected due to global warming, increased CO_2, increased anthropogenic nitrogen sup-

*Corresponding author: nealep@si.edu

Publisher: Inter-Research · www.int-res.com

ply, and changes in irradiance (including increased UV-B radiation) (Beardall et al. 2009). Global warming is important to marine ecosystems as it induces changes in circulation (affecting spatial distributions) and stratification (affecting average irradiance and vertical nutrient flux) (Boyd & Doney 2002). The actual increase in temperature, however, has minor metabolic significance (Thomas et al. 2012). The oceans are absorbing most of the anthropogenic emissions of CO_2, which not only affects the quantity and speciation of the dissolved inorganic carbon in the ocean, but also lowers the pH, most directly impacting phytoplankton, other aquatic plants, and calcifying organisms (Feely et al. 2009). The supply of other inorganic nutrients (mainly nitrogen) to the coastal ocean is also increasing due to agricultural practices and coastal development (Rabalais et al. 2009).

The other resource that sustains microbial (and most other) life in the ocean is solar irradiance. The availability of photosynthetically active radiation (PAR, 400 to 700 nm) to phytoplankton in the surface mixed layer is determined by the balance between surface forces causing vertical mixing vs. stratification (in turn affected by global warming), and future shifts in this balance are expected to be regionally dependent (Gargett & Marra 2002). Concurrently, there has been a latitudinally variable increase in UV radiation (UVR), specifically the shorter wavelength and more damaging UV-B (290 to 315 nm for incident solar radiation), related to the depletion of stratospheric ozone (Weatherhead & Andersen 2006). Although emissions of chlorofluorocarbons (CFCs; the anthropogenic factor that caused ozone depletion) has been curtailed, ozone recovery has slowed in many areas, particularly the Southern Hemisphere (Weatherhead & Andersen 2006). Severe ozone depletion ('ozone holes') continues to occur in the Antarctic and periodically in the Arctic (WMO 2011). This slower recovery is attributed to the strong interaction between stratospheric ozone depletion and changes in climate induced by increasing greenhouse gases (McKenzie et al. 2011). Each of these environmental factors has the potential to strongly influence marine microbial communities, and these responses are explored in more detail in several recent reviews (Riebesell et al. 2008, Doney et al. 2012, Winder & Sommer 2012, Caron & Hutchins 2013).

As the evidence for environmental changes has become more established, it has also been realized that simultaneous changes in several variables may not result in a simple additive responses relative to that occurring with any one variable alone (Boyd & Hutchins 2012). As variables change in tandem, there can be either synergistic, antagonistic, or independent effects (Folt et al. 1999). Manipulative experiments are one approach towards examining the interactive effects of global change variables. Experiments using intact communities spanning multiple trophic levels are the best methods for understanding whole ecosystem responses to multiple interacting factors (Litchman et al. 2012). In terms of the interactions between the global change factors most impacting marine pelagic microbes (i.e. elevated CO_2, nutrients, and irradiance), investigations to date have mainly focused on single species or natural assemblages screened to remove macrozooplankton. The interaction of nutrient availability and elevated CO_2 has been examined for several phytoplankton species in culture. Responses to the 2 variables were relatively independent in the diatom *Phaeodactylum tricornutum* (Li et al. 2012): growth rate, pigment contents, effective quantum yield, and cell size responded strongly to nutrients, but enhancing CO_2 availability did not significantly affect the response to nutrients. In a continuous culture experiment using an enrichment assemblage of freshwater phytoplankton and bacteria, enhancing CO_2 increased primary production and dissolved organic carbon (DOC) concentration with no change in algal biovolume, whereas increased nutrients increased carbon biomass but had no effect on DOC (Song et al. 2014). One direct interaction of enhanced CO_2 (and lower pH) and nitrogen availability is that decreased pH slows denitrification, resulting in a higher ammonia:nitrate ratio. This compounded the negative effects of acidification on the calcification rates in a cultured strain of the phytoplankter *Emiliana huxleyi* (Lefebvre et al. 2012). Enhanced CO_2 effects also interact with those of irradiance on phytoplankton physiology, improving photosynthetic efficiency at low light, but increasing sensitivity to photoinhibition by PAR (Gao et al. 2012) and UVR (Sobrino et al. 2008). To date, the concurrent manipulation of all 3 variables (elevated CO_2, nutrient enrichment, and irradiance) has not been experimentally attempted, neither for single species nor for plankton communities.

The semi-enclosed nature of the Mediterranean Sea makes it more sensitive to natural and anthropogenic variations in fluxes (air–sea and freshwater) and water flows. Seawater temperatures, stratification of the water column, and inflows of fresh water and nutrients are expected to vary more in Mediterranean coastal waters than other marine areas (Rabalais et al. 2009). In particular, the relatively high alkalinity of the Mediterranean Sea entails a higher

capacity for absorbing anthropogenic CO_2 than other parts of the ocean (Schneider et al. 2007). Concordantly, Touratier & Goyet (2009) demonstrated that the anthropogenic CO_2 concentrations in the Mediterranean Sea are much higher than in the Atlantic Ocean. If this is the case, the pH drop in the Mediterranean Sea could be relatively large compared to that predicted to occur globally (i.e. 0.5 pH unit for the year 2100 according to Caldeira & Wickett 2003 and IPCC 2013). Acidification could produce a reduction in phosphate concentration and alteration of the equilibrium between NH_4 and NH_3, especially in Mediterranean coastal zones (CIESM 2008). Furthermore, the Alboran Sea (the most western basin of the Mediterranean Sea) is subject to strong anthropogenic impacts. Surface temperatures in the northern Alboran Sea increased at a rate of 0.05°C yr^{-1} from 1992 to 2008 (Vargas-Yáñez et al. 2002). Mercado et al. (2007) found that this change could be related to inter-annual variability in the atmospheric forcing that produced a reduction in intensity of the wind-induced coastal upwellings. Furthermore, Mercado et al. (2012) described high phosphate concentrations in the Bay of Málaga, whose probable origins are the discharges of urban residual waters.

Experiments examining the effects of multiple changing environmental factors (singly or in combination) on planktonic communities of the Mediterranean Sea are scarce despite their sensitivity to global change. Climate change effects have been demonstrated in the Western Mediterranean for temperature (Vargas-Yáñez et al. 2002) and acidification in the strait of Gibraltar (Huertas et al. 2009). The interaction of warming and increased UVR was investigated in a mesocosm experiment using the NW Mediterranean coastal plankton community in the Thau Lagoon. Increased temperature favored microzooplankton and copepods more than their bacterial and algal prey, but the community was little affected by increased UV-B (Vidussi et al. 2011). The interactions of nutrients, temperature, and UVR were evaluated for plankton up to 1 µm (no micrograzers) and up to 6 µm (with micrograzers) in manipulative microcosm experiments with the Thau Lagoon microbial community (Bouvy et al. 2011). Generally, manipulation of bottom-up factors changed microbial growth rates, but the presence or absence of micrograzers was the most important determinant of carbon biomass. Calbet et al. (2012) studied the effects of light availability on mixotrophy and microzooplankton grazing in an oligotrophic plankton food web in a mesocosm study in the Eastern Mediterranean waters, and observed that the decrease in nutritional quality of phytoplankton in mesocosms at high irradiance (higher C:chlorophyll ratios) was not reflected in a lower final abundance of grazers (both micro- and mesozooplankton). The authors pointed out that further work is needed in order to better understand the effect of light availability on Mediterranean aquatic food webs.

Here, we report on the results of a factorial manipulation of a natural plankton community up to microplankton size (i.e. <200 µm) sampled from the Mediterranean coastal ecosystem of the Alboran Sea. We investigated the joint effects of elevated CO_2, nutrient enrichment, and irradiance (including UVR). The result are reported in a series of 4 articles. In this first article, we present an overview of the variation of physico-chemical variables in the experiment and the coupled variation in biomass characteristics, both between and within trophic levels. Later articles in the series present more detailed results on rates of production (Mercado et al. 2014), changes in size distribution and taxonomic composition (Reul et al. 2014) and indicators of physiological condition (Sobrino et al. 2014) (all this Theme Section).

MATERIALS AND METHODS

Experimental setup

The experiment was part of the Group for Aquatic Productivity, 9th international workshop (see general information on the workshop at www.gap9.uma.es/INDEX.PHP/). Over a 7 d period, we measured the variation of the characteristics of phytoplankton and bacterioplankton incubated under 8 treatments, representing the full factorial combinations of 2 levels each of nutrient concentrations, CO_2 supply, and solar radiation exposure as shown in Table 1. The water was incubated in microcosms consisting of 20 l bags made of UVR-transparent low-density polyethylene (LDPE) ('cubitainers') that were suspended in 4 large volume tanks (approximately 800 l each). Six microcosms floated in each tank, tethered to an overhead support to maintain position near the center to minimize shading. There were 3 replicate microcosms per treatment, with 1 pair of treatments located in each tank. Two tanks were 'high light' (HL, single layer of nylon screen) treatments and 2 'low light' (LL, double layer of nylon screen) treatments, giving a total of 24 microcosms distributed over 4 tanks. Tank water was circulated through coolers (Aqua-Medi-Titan-500) to maintain close to ambient temperature at the sampling site (20 to 22°C).

A total of ca. 900 l of seawater was collected from the surface in the western Mediterranean (Alboran) Sea, about 2 km offshore from the Instituto Español de Oceanografia (IEO) in Fuengirola, Spain (approximate sampling position 36.54° N, 4.60° W) on 15 September 2012 (Day –1). Depth profiles of temperature, salinity, and irradiance (multiparameter meter HANNA HI 9828) and chlorophyll *a* (chl *a*) were measured. Multiple casts were made over a 3 h period (11:00 to 14:00 h local time). The seawater was screened through a 200 µm mesh as it was collected to remove mesozooplankton. Mesozooplankton were excluded because the volume and duration of our experiment was not appropriate for studying their dynamics, and to avoid increased variability between replicate microcosms due to uneven grazing effects. After screening, the collected seawater was combined in a mixing tank at IEO. Microcosms were filled from the mixing tank on Day –1 and kept inside the temperature-regulated tanks with regular aeration overnight until CO_2 aeration began on 16 September at 09:00 h, when the initial (Day 0) sample was taken from water remaining in the mixing tank. Experimental sampling continued daily from 17 through 22 September (Days 1 through 6).

Nutrient additions to the HN treatments were performed in 2 pulses. The first pulse was made on Day 0 with a combination inorganic and organic nutrients simulating the effects of coastal eutrophication as previously described by Martínez-García et al. (2010) (concentrations are specified below). The strategy was to have the availability of inorganic nitrogen and phosphorus at a 12:1 ratio (nitrogen deficient with respect to the Redfield ratio) with additional nitrogen added as amino acids. Nutrient levels were checked on Day 2, and a second addition of P alone was made again based on a target ratio of 12:1. The actual ratios obtained were somewhat lower (see details in 'Results').

Table 1. Treatment combinations for the microcosms: HC = high CO_2 (elevated to 1000 ppmv); LC = low CO_2 (ambient air); HN = high nutrient addition; LN = low nutrient (no nutrient addition); HL = high light (61% irradiance level); LL = low light (32% irradiance level)

Treatment no.	CO_2 supply	Nutrients	Solar irradiance
1	HC	HN	HL
2	HC	LN	HL
3	HC	HN	LL
4	HC	LN	LL
5	LC	HN	HL
6	LC	LN	HL
7	LC	HN	LL
8	LC	LN	LL

All microcosms were aerated at a flow rate of ca. 100 ml min^{-1} with either ambient air (LC, low CO_2) or air that was enriched with CO_2 to a level of 1000 ppmv (HC, high CO_2). Flow rate was controlled with individual flow meters (Aalborg), and CO_2 supply was provided from a gas tank.

Tanks were covered with either a single (HL) or double (LL) layer of nylon window screen. These (together with the shading from the closed sided tanks) resulted in an effective irradiance level of 61 and 32% of incident for HL and LL, respectively. The screens and microcosm materials (LDPE) transmit the full solar spectrum (UVR + PAR).

A list of variables sampled and the frequency of sampling is shown in Table 2. We have divided the presentation of the results of the overall experiment into a series of 4 reports, and Table 2 identifies which report in the series presents the results of each measurement.

Measurements

Incident irradiance

Spectral irradiance at 305, 320, and 380 nm (10 nm bandwidth) and PAR was recorded near the tanks using a BIC radiometer (Biospherical Instruments). Average irradiance was recorded every minute through the day. The BIC was last calibrated in 2005; therefore, instrument response was checked by comparison with spectral irradiances calculated using a radiative transfer model (STAR, System for Transfer of Atmospheric Radiation; Ruggaber et al. 1994) using the default settings for maritime environments and total column ozone from satellite measurements (OMI). Previous comparisons have shown that this approach results in good agreement between STAR predictions in the UV and measurements under clear sky conditions (Neale et al. 2001, 2005). Scalar ($4 - \pi$) PAR irradiance was also measured in the incubation tanks and at the sampling station with a Licor LI-193SA spherical quantum sensor.

Temperature

Temperature was continuously recorded using HOBO Pendant UV temperature/light loggers (Onset Computer) deployed in the experimental tanks (the 2 HL tanks). Spot readings with a hand-deployed digital thermometer were taken from time to time to monitor tank temperature and adjust cooling capacity if necessary.

Table 2. Variables sampled, frequency, and where the results are presented. I: This study; II: Mercado et al. (2014); III: Reul et al. (2014); IV: Sobrino et al. (2014)

Measurement type	Frequency	Where presented
pH, temperature, salinity	Daily	I
Dissolved inorganic carbon/pCO_2	Daily	I
Nutrients (autoanalyzer)	Daily	I
Incident irradiance (BIC)	Daily	I
Chromophoric dissolved organic matter (CDOM)	Days 0, 2, 4, 6	I
Bacterial production and counts	Days 2, 4, 6	I & II
Low temperature emission spectroscopy	Days 0, 2, 4, 6	I
Chlorophyll concentration (total)	Daily	I
>0.7 µm and >20 µm	Days 0, 2, 4, 6	I
Particulate organic carbon (POC) and nitrogen (PON), dissolved organic carbon (DOC)	Day 6	I & II
C and N uptake (total and <20µm)	Days 2, 4, 6	II
Fractionated ^{14}C phytoplankton uptake (>0.2 µm, >20 µm)	Days 0, 2, 4, 6	II
Respiration (Optode)	Days 0, 2, 4, 6	II
Transparent exopolymers (TEPs)	Days 2, 4, 6	II
Species composition (microscopy)	Days 0, 2, 4, 6	III
Species composition (Chemtax-HPLC)	Days −1, 6	III
Species composition and size structure (flow cytometry and flow cam)	Daily	III
Species composition and size structure (Fluoroprobe)	Daily	III
PAM measurements	Daily	IV
Reactive oxygen species (ROS)	Days −1, 0, 2, 4, 6	IV
Cell viability (Esterase activity-FDA)	Days −1, 0, 2, 4, 6	IV
Cell viability (Cell death-SYTOX Green)	Days −1, 0, 2, 4, 6	IV
Cyclobutane-pyrimidine-dimers CPD's (DNA damage)	Days −1, 0, 4, 6	IV
Total, particulate and dissolved ^{14}C phytoplankton uptake (EOC-PER)	Days 0, 2, 4, 6	IV
Cell viability-permeability (cell digestion assay)	Days 2, 4, 6	IV

Salinity, pH and total dissolved inorganic carbon

Salinity, pH and total dissolved inorganic carbon (TDIC) were the first samples collected during the daily sampling. pH and salinity were measured in all microcosms using a pH-meter (CRISON Basic 20+) calibrated regularly using NBS (National Bureau of Standards) buffers and a conductivity meter (CRISON 524). The accuracy of the conductivity meter and pH meter was ±1.5% and ±0.01 pH units, respectively. TDIC samples were filtered through 0.2 µm nitrocellulose filters and sealed into 10 ml acid-washed serum glass vials that were capped without headspace. The samples were analyzed using an infrared gas analyzer (LiCOR 7000) and the partial pressure of CO_2 in the water samples (pCO_2) was calculated from salinity, temperature, pH and DIC measurements using the program 'csys.m' from Zeebe & Wolf-Gladrow (2001).

Phytoplankton pigments and biomass

Water samples (250 ml) were collected daily from each microcosm to determine total chl *a* concentration. Samples were filtered through fiberglass filters with a 0.7 µm nominal pore size (Millipore® APFF). Pigments were extracted with 90% acetone for 24 h in a dark and cold (<4°C) chamber. Total chl *a* concentration corrected for phaeopigment was calculated from the fluorescence of the extract before and after acidification, following the method of Yentsch & Menzel (1963). Fluorescence was measured by means of a Perkin Elmer fluorometer (LS50B) previously calibrated with pure chl *a* from spinach (Sigma). For size-fractionated chl *a*, additional water samples (250 ml) were collected every other day (Table 2), filtered through 20 µm nominal size pore filters (Millipore®), and analyzed following the same method. On Day 6, additional samples (500 ml) were collected, filtered on precombusted Whatman GF/F filters and analyzed for particulate organic carbon (POC) and particulate organic nitrogen (PON) using methods described by Mercado et al. (2014).

Bacterial abundance

For the counts of heterotrophic picoplankton (HPP), 50 ml of water from each treatment was fixed with a paraformaldehyde and glutaraldehyde solution made up in phosphate buffered saline to a final concentration in the sample of 1:0.05% w/v, respectively (Marie et al. 1997). Subsamples between 10 and 20 ml (depending on microbial biomass) were filtered through 0.2 µm pore size black filters (Nuclepore™) at low pressure. A quarter of the filter was stained with DAPI (Porter & Feig 1980) and counted in an inverted Zeiss III RS epifluorescence microscope (1250×); fluorescence of cells was observed

by using a standard filter set for UV excitation (MacIsaac & Stockner 1993). At least 1000 individuals and 10 fields were counted in each treatment.

Aerobic anoxygenic photoheterotropic (AAP) bacteria

To determine the abundance of photosynthetic AAP bacteria, fluorescence emission spectra were measured at low temperature (77K) using a portable instrument as described by Prásil et al. (2009). For each treatment, 100 ml of water was filtered through 2 layers of Whatman GF/F filter. The cut filters were placed into a sample holder, cooled by liquid nitrogen, and sequentially excited by spectrally narrow illumination from 1 of 6 LEDs (390, 455, 470, 505, 530, and 590 nm). The emission was recorded in the 600 to 1000 nm spectral region, with 1 nm resolution and 300 ms integration time. Background spectra (measured with a blank GF/F filter) were subtracted, and relative abundance of photosynthetic bacteria was estimated from the height of the bacteriochlorophyll *a* (bchl *a*) emission band centered at 885 nm. For this purpose, we analyzed spectra excited at 530 nm. Because the intensity of the bchl *a* emission from anoxygenic bacteria was <2% of the emission of oxygenic phytoplankton around 690 nm, the tail from this chl *a* emission formed significant part of the 885 nm signal. Therefore, the 885 nm emission due to chl *a* was numerically estimated and subtracted from the signal. Statistical analysis was performed using Statistica v.10 (StatSoft).

Phytoplankton taxonomy

The taxonomic composition of phytoplankton was determined from each treatment at initial time (Day 0) and every 2 d until the end of the experiment (Days 2, 4 and 6). Samples were collected in 120 ml opal glass bottles and fixed with acid Lugol's solution at a final concentration of approximately 3%, to be later processed following the Utermöhl Technique (Utermöhl 1958). A volume of 50 or 25 ml was settled in a chamber for 24 h, and then analyzed by means of a Nikon Eclipse TS100 inverted microscope. A sufficient number of fields (at least 2 transects) were counted at 200× magnification until at least 100 individuals of the most abundant species or genera were registered (Ros & Miracle 1984). Small flagellates were counted using a 600× magnification. Furthermore, the bottom of the chamber was scanned at 40× in order to count the larger cells. The smallest size limit for microscopic enumeration was established at 3 µm. The abundance of smaller cells was measured using FACScan flow cytometer after screening through 20 µm mesh (for details of settings see Reul et al. 2014). Phytoplankton organisms were identified to genus or species level when possible following species nomenclature of Tomas (1997). Only selected group-level microscopic results and flow cytometry totals for cells <2 µm (picophytoplankton) are reported here; more detailed taxonomic and size information is presented in Reul et al. (2014).

Inorganic nutrients

For inorganic nutrient analysis, 3 subsamples of approximately 10 ml were collected in 12 ml polystyrene tubes rinsed twice with sample water and immediately frozen at −20°C until analysis. Before analysis, samples were thawed in a bath of warm water, kept in the dark and analyzed within 1 h. Inorganic nutrient concentrations were analyzed by segmented flow analysis (SFA) using a Bran-Luebbe AA3 autoanalyzer following the methods described by Grashoff et al. (1983). The detection limits of the inorganic nutrients were 0.03 µM for nitrates, 0.01 µM for nitrites, 0.02 µM for phosphates, 0.05 µM for silicates, and 0.06 µM for ammonia.

DOC

Water samples (50 ml) were collected from each microcosm on Day 6 (final day), filtered through 0.2 µm cellulose acetate filters (Whatman), and stored in acid-washed and baked glass bottles at 4°C in darkness until analysis (ca. 10 wk after the experiment). Samples were then transferred into acid-washed and baked 25 ml glass vials and covered by baked foil. DOC was measured in a Shimadzu TOC-L analyser using the non-purgable organic carbon (NPOC) method. Samples were sparged for 2.5 min with synthetic zero air (79% N and 21% O_2) and acidified with 1.5% HCl. A 5 point calibration curve with potassium-hydrogen-phthalate (KHP) (Sigma) ranging between 1 and 10 ppm was used as organic carbon standard. Two distilled water blanks were run between samples to ensure that carryover between samples was negligible, and 5 technical replicates of each sample were analyzed. The average coefficient of variation for quintuplicate DOC analysis was 1 to 2% of the mean.

Chromophoric dissolved organic matter (CDOM) absorbance

Sample water filtered over 0.2 µm filters (cellulose acetate) from Days 0, 2, 4, and 6 was stored in high density polyethylene (HDPE) tubes for 1 to 2 d until analysis. Absorbance scans were performed on a Cary 100 spectrophotometer using 2 cm pathlength quartz cuvettes and a purpose-built cuvette holder. The wavelength range was 250 to 750 nm, with wavelength interval and bandwidth of 1 nm. The instrument was baselined on milli-Q grade distilled water. A blank was run every 3 scans, and if serious departure of the blank from baseline was observed, the instrument was re-baselined. The average of the blanks before and after a set of scans was subtracted from the raw data to obtain corrected measured absorbance.

Overall, CDOM absorbance was low (as expected) for the near-oligotrophic status of the coastal Mediterranean sample. Although samples were warmed to room temperature before analysis, small departures from baseline around 750 nm were occasionally noted. These were attributed to the temperature-dependent water absorption coefficient in the infrared (Pegau et al. 1997); therefore, it was assumed that absorbance at 700 nm was zero. Absorption coefficient was calculated as:

$$a(\lambda) = 2.303 \times [A(\lambda) - A(700)] / 0.02$$

where a = absorption coefficient (m^{-1}), A is Cary-measured optical density, and λ is wavelength 250 to 700 nm. Here, we present the absorbance at 250 nm (a_{250}) which was the maximum in all cases, and the slope ratio which was based on the ratio of slopes (s275:s350) of ln(a) vs. wavelength for the spectral ranges of 275 to 250 nm (s275) and 350 to 400 nm (s350) following the approach of Helms et al. (2008).

ANOVA

Statistical significance of treatment effects was tested using repeated measures ANOVA. Calculations were performed using the SAS v.9.2 generalized linear model (GLM) procedure with main effects, time (repeated measure), and interaction terms. Results of univariate significance tests are reported since Mauchly's criteria for sphericity were met (chi-square not significant) for all variables except picophytoplankton log abundance, for which the reported significance is based on MANOVA and exact F-test.

RESULTS

Source water

The depth at the sampling station was 45 m. The temperature profile taken around midday (11:00 h LT) showed near-surface stratification, with the temperature dropping from 22.6 to 21.1°C over the upper 2 m (Fig. 1A). Salinity was 36.0 psu. Below this was a layer of weak stratification and a secondary temperature step between 20.6 and 19.2°C at 8 m. The PAR depth profile showed a moderate transparency, with a PAR attenuation coefficient (slope of ln(PAR) vs. depth) of 0.31 m^{-1} (Fig. 1B). Chl *a* concentration was in the mesotrophic range, around 1.8 µg l^{-1} in the 2 to 8 m layer, but was substantially lower at the surface (0.8 µg l^{-1}) (Fig. 1C). Based on the estimated attenuation coefficient, plankton in the upper 1 m would have been experiencing about 85% of incident (just below surface) irradiance, suggesting that the assemblage used for the experiment was under high irradiance stress at time of sampling. On the other hand, before being 'trapped' by near-surface stratification, the assemblage should have been high-light acclimated. This assumes that over the longer term (days-week) mixing was in the range of 5 to 8 m, resulting in an average PAR exposure 51 to 37% of incident, respectively.

Physical and chemical variables

Irradiance

Sky conditions during the workshop were variable, with some days having mist and fog in the morning and sun or partially overcast conditions in the afternoon, while clear sky conditions prevailed on other days (Fig. 2). Clear sky weather on Day −1 (15 September 2012, data not shown) was chosen to perform a comparison between the BIC-measured and STAR-calculated irradiances. Model predictions and measurements were in good agreement at 380 nm and for PAR, but measurements were about 30% lower than model estimates at 305 and 320 nm. To correct for the underestimates by the BIC instrument, raw values were divided by the slope of a linear regression between BIC measurements and STAR-calculated irradiances at each wavelength over the course of the day on 15 September (the intercept was not significantly different from zero). The estimated slopes were 0.740 at 305 nm and 0.708 at 320 nm.

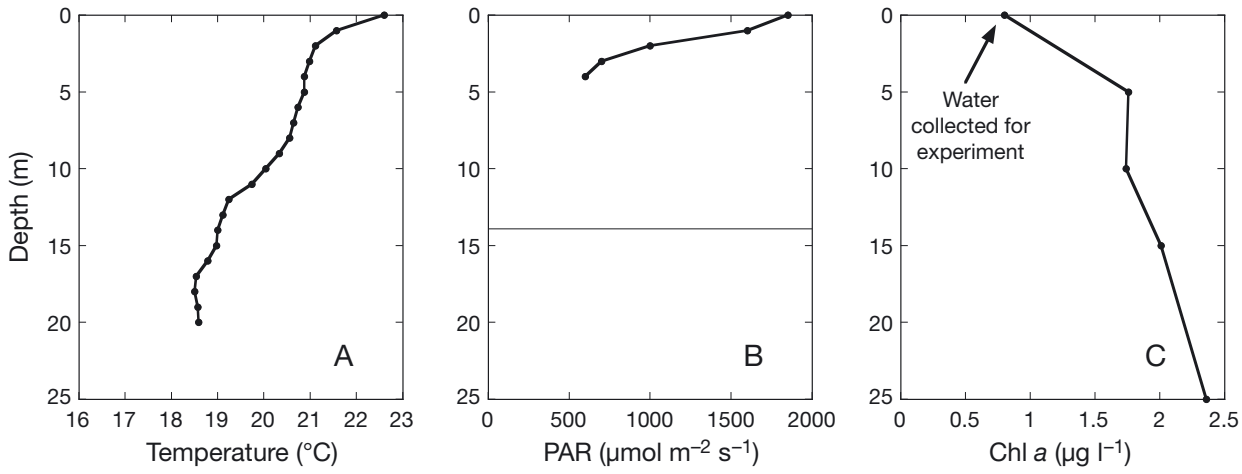

Fig. 1. Depth profiles of (A) temperature, (B) photosynthetically active radiation (PAR), and (C) total chl *a* at the coastal Alboran Sea station sampled on 15 September 2012 to obtain source water for the microcosm experiment. Horizontal line in (B) indicates the Secchi depth. Arrow in (C) indicates that water for the experiment was collected at the surface

To estimate the full spectrum of incident UVR and PAR spectral irradiance during the experiment, a modification of the procedure by Neale et al. (2005) was followed. STAR spectra were calculated for the full daylight period of each day at 15 min intervals. Clear sky spectra at the 1 min intervals of BIC measurements were estimated by linear interpolation. To correct for cloudiness, the clear sky spectra were multiplied by an 'atmospheric correction', namely the ratio of the BIC measurement at 380 nm to the STAR-calculated irradiance at 380 nm (wavelength of best agreement between STAR and BIC under clear sky). The validity of the atmospheric and calibration corrections was supported by the close correspondence of BIC-measured and corrected STAR irradiance at 320 nm (Fig. 2B).

Average (±range) midday (solar noon ± 2 h) PAR in the microcosms after adjusting for transmission of the cubitainer and screen(s) was 539 and 232 µmol m^{-2} s^{-1} for HL and LL, respectively. Day to day, the midday average varied by 50% around this grand mean due to changing sky conditions, ranging between 227 and 793 µmol m^{-2} s^{-1} for HL, and between 119 and 416 µmol m^{-2} s^{-1} for LL. Total UVR exposure (290 to 400 nm) for this midday period ranged from 7.4 to 22.7 W m^{-2} (HL), and 3.9 to 11.9 W m^{-2} (LL).

Temperature and salinity

The microcosms were immersed in tanks filled with fresh (tap) water that was circulated to maintain tem-

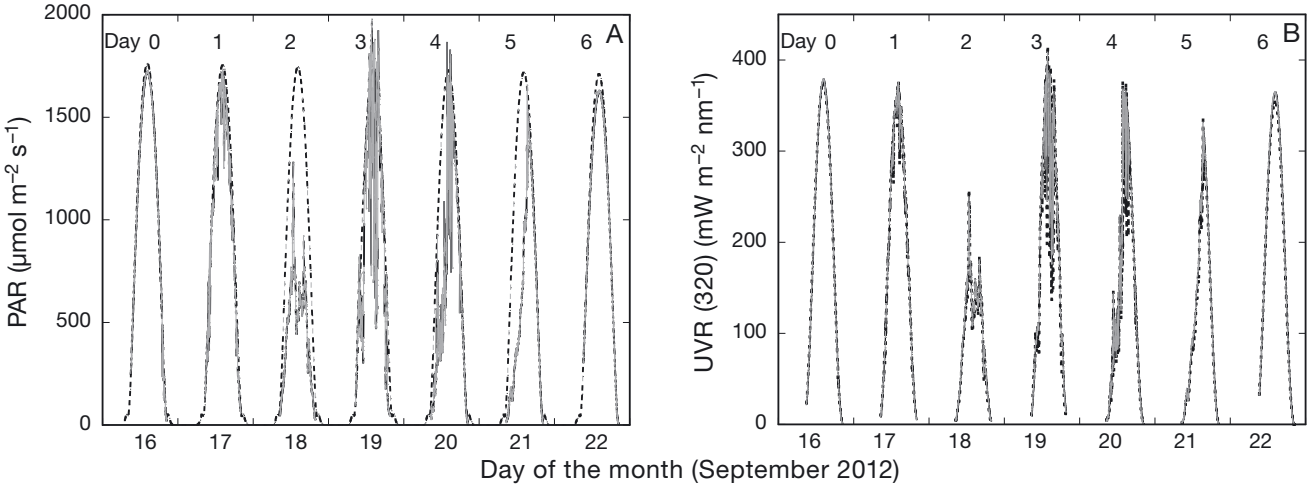

Fig. 2. Variation of (A) photosynthetically active radiation (PAR) and (B) UVR during the WG1 experiment. Dashed line in (A) shows the expected value for clear sky conditions based on the System for Transfer of Atmospheric Radiation (STAR) radiative transfer model and (B) the STAR estimated spectral irradiance at 320 nm after applying a atmospheric correction; solid grey line in (A) shows the actual recorded irradiance for PAR (µmol m^{-2} s^{-1}) and (B) a representative wavelength (320 nm) of spectral UV irradiance (mW m^{-2} nm^{-1})

perature. Water temperature in the microcosms was kept between 21 and 22°C corresponding to *in situ* conditions at the sampling site. On Day 3 (19 September; sunny day), there was a somewhat greater (1.4°C on average) difference between daily minimum and maximum temperatures. Salinity also remained stable around 36 ± 0.18 psu.

Other chemical parameters were subject to manipulation and thus varied with time. The variation of key chemical and biological parameters for each treatment is shown in Fig. 3, and the following summarize the temporal pattern for each.

Nitrogen and phosphorus

The sample water collected for the experiment on Day −1 was low in nutrients as is typical for this region of the Mediterranean (Ramírez et al. 2005). Nitrate+nitrite was 0.6 µM, ammonium 0.2 µM, and phosphate was 0.14 µM. The dissolved inorganic nitrogen (DIN) to soluble reactive phosphorus (SRP) ratio was 5.8, indicating strong nitrogen limitation. In the LN treatments, concentrations declined to near the detection limit by Day 2 for phosphate and nitrate+nitrite (Fig. 3A,B) as well as ammonium (data not shown). For the HN treatments, 3 µM nitrate and 0.2 µM phosphate was added on Day 0 to bring the initial N:P ratio to 11:1. Following the approach of Martínez-García et al. (2010), we also added a mixture of glucose and amino acids, each equimolar with the nitrate addition. By Day 2, an appreciable amount of nitrate remained in the enriched treatments, but virtually all the phosphate had been consumed (Fig. 3B). Indeed, on the day after the addition the average phosphate concentration in the HN microcosms was 0.12 ± 0.02 µM, indicating that most P uptake had occurred in the first 24 h after addition. However, the extent of P depletion was not realized until Day 2 of the experiment. Additional phosphate was added on that day as needed in order to restore a near 11:1 N:P ratio. Nitrate and phosphate showed only modest consumption from Day 2 to Day 6 (Fig. 3A,B).

The main limiting nutrient in the high nutrient treatments by Day 4 seems to have been silicate. It was 1.2 µM in the starting water, declined to around 0.6 to 0.8 µM by Day 2, and was near detection limit in all treatments for Days 4 through 6 (Fig. 3C). These concentrations are consistent with silicate limitation of diatoms in the HN treatments on Days 4 through 6. The depletion of silicate was connected with the development of a diatom bloom (more details in 'Phytoplankton abundance' below, also see Reul et al. 2014).

pCO_2 and DIC

In general, pCO_2 reflected the experimental targets of ca. 1000 (µatm or ppmv) in the enhanced CO_2 treatments versus 400 to 500 µatm in the treatments aerated with ambient air (Fig. 3D). Average DIC was also enhanced from 2321 to 2498 µmol l^{-1} comparing the LC and HC treatments, respectively (see Appendix). However, further enhancement in pCO_2 occurred (up to 2000 µatm) in the HC HL treatments on Day 4. In the ambient air microcosms, pCO_2 started around 500 µatm and decreased somewhat with time.

CDOM and DOC

Full spectral absorbance of CDOM from 250 to 700 nm was measured on filtrates (<0.2 µm pore size). For simplicity, Fig. 3E shows the maximum absorbance, which was at 250 nm (a_{250}) in all cases. From Day 0 to Day 2, there was a large increase in absorbance in all treatments relative to the initial sample, with a decreasing trend in later samples. The rate of decrease differed between the HC (faster) and LC (slower) treatments. The spectral slope ratio was estimated as described in 'Materials and Methods' in order to obtain information on CDOM quality and those processes controlling its concentration. The slope ratio of the Day 0 water was 1.7, which is characteristic of mesotrophic coastal waters (Helms et al. 2008). On Day 2, the ratio increased to 2.2 ± 0.3. Increases in slope ratio are often interpreted as an indication of photobleaching; however, in this case it was coupled with an increase in a_{250} suggesting that instead it was related to a release of material with high short wavelength absorbance. This could be related to the release of low molecular weight material, perhaps of cellular origin. Also consistent with a limited contribution of photobleaching is that a similar increase in slope ratio occurred in both HL and LL treatments (data not shown). Afterwards, the ratio decreased again, to 1.4 ± 0.2 on Day 4 and 1.6 ± 0.3 on Day 6. The decrease on Day 4 was significantly greater for HC than LC (*t*-test, $p < 0.001$). Decreases in slope ratio coupled with decreases in absorbance are consistent with microbial uptake.

CDOM is a subset of total dissolved organic matter which was measured as DOC. Because of volume constraints, this component was only sampled on Day 6. Although by Day 6 CDOM was at or below initial levels (Fig. 3E), DOC was significantly higher than its initial concentration (Fig. 4A). The increase was par-

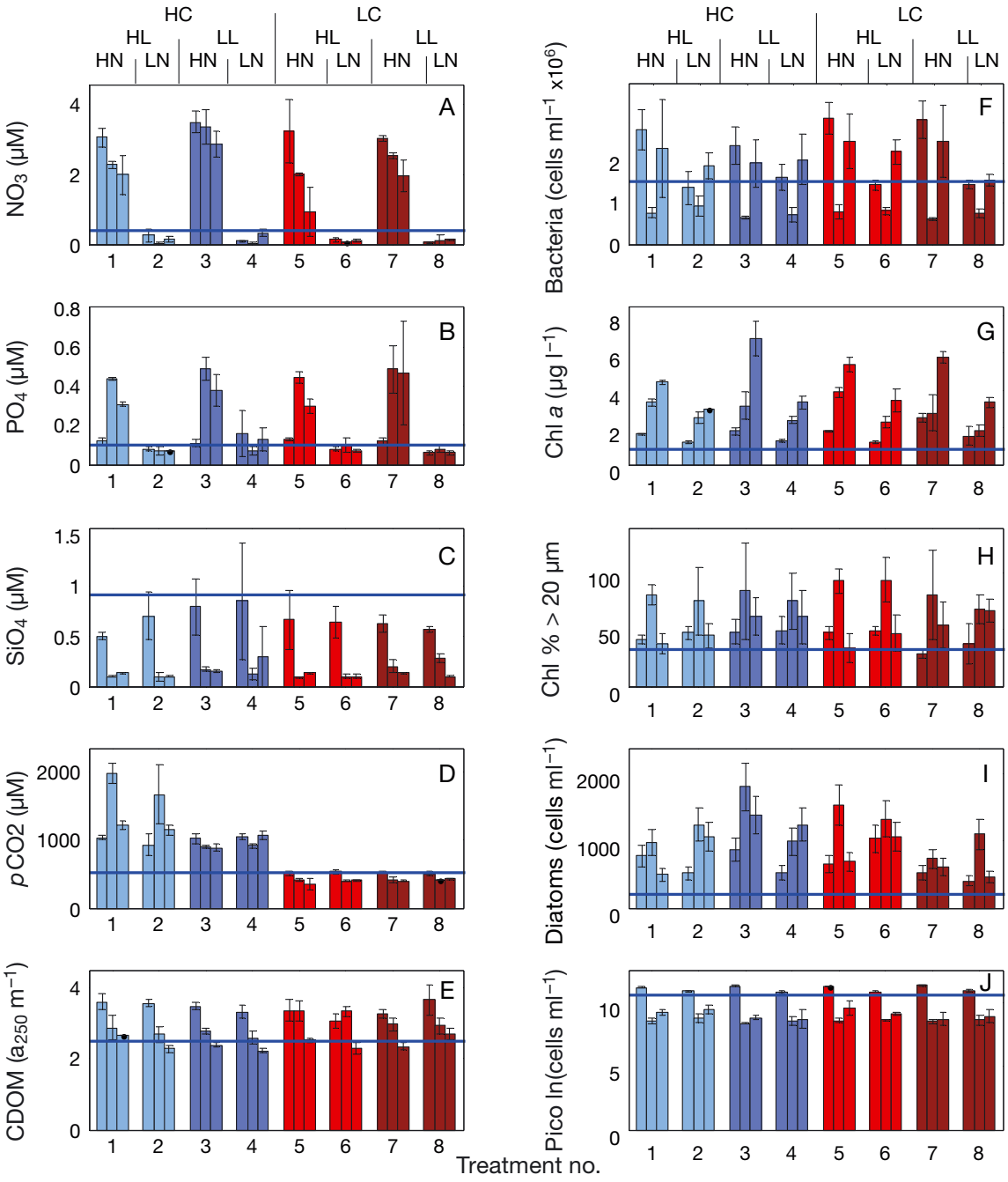

Fig. 3. (A–J) Time variation of key variables in the WG1 microcosms. Average ± SD (n = 3 replicate microcosms) is shown for each of 8 treatments, with treatment key shown at the top (see Table 1), and treatment types color-coded to aid interpretation. The 3 bars in each group correspond to the Day 2, 4, and 6 data; horizontal lines indicate value for Day 0. Diatom abundance was determined for only 1 replicate of each treatment, so error bars show an estimated ±5% uncertainty in this measurement. Note log-scale *y*-axis for (J) (picophytoplankton abundance)

ticularly large, although variable, in the HC treatments. Since CDOM was near initial levels, this dissolved material must be largely non-chromophoric (e.g. molecules lacking in aromatic or conjugated structures associated, for example, with humic materials). Consistent with this is the specific ultraviolet absorbance (SUVA), a ratio between absorbance and DOC concentration, which is conventionally calculated at 254 nm. SUVA averaged 0.78 in the HC treatments and 1.3 in the LC treatments. A SUVA <1.0 is considered characteristic of a very low aromatic content (Helms et al. 2008).

Biological variables

POC and PON

Transfer of the initial sample to the experimental microcosms stimulated growth in all treatments. This is shown most concretely by the increase in particulate organic material, measured either as carbon (POC, Fig. 4B) or nitrogen (PON, Fig. 5A), both of which had increased significantly above initial concentrations by the time sampling occurred on Day 6. Both at least doubled above the Day 0 level, except in the least 'resourced' treatment (LC LN LL) in which, nevertheless, POC and PON increased substantially (Figs. 4 & 5). The increase in PON was highest in the HN treatments, leading to a considerable drop in the C:N ratio of particulate material from the initial value of 10 (Fig. 5B) The average C:N ratio in the HN was 7.2, compared to a Redfield ratio 6.6, which is consistent with a large contribution from growth of nutrient sufficient cells. Smaller increases in PON and decreases in C:N occurred in the LN and LL treatments.

Bacterial abundance

Growth of bacterioplankton accounted for part of the increase in organic particulates. Their growth was strongly stimulated in the initial 2 d in the HN treatments (Fig. 3F). This growth was particularly high in HN treatments, presumably stimulated by the organic nitrogen amendment combined with inorganic P, and resulting in the large decrease in PO_4 despite little change in phytoplankton by Day 2 (more detail in next section). This initial bacterial bloom had dissipated by Day 4, declining below initial abundance followed by a resurgence in bacterial abundance on Day 6 (Fig. 3F). In the LN treatments, there was no initial bloom but bacterial abundance also experienced a decline by Day 4 followed by a resurgence on Day 6. There were no marked differences in these responses between HC and LC treatments.

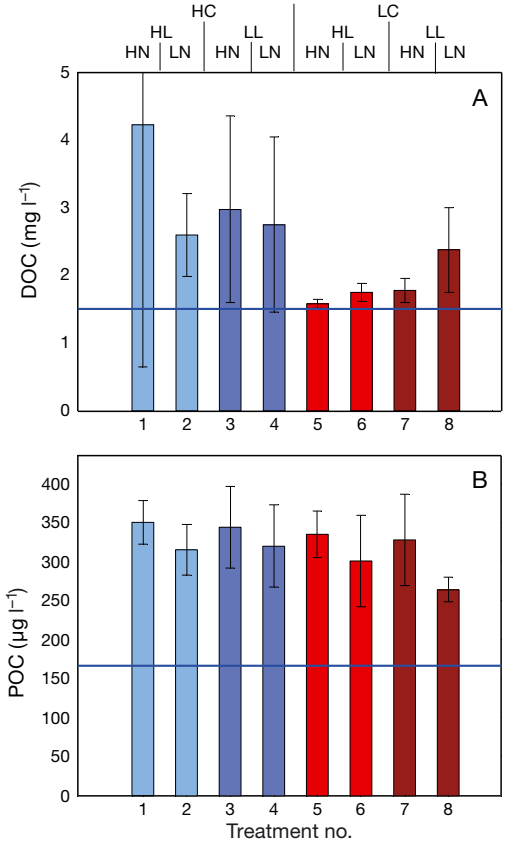

Fig. 4. Measurements of (A) dissolved and (B) particulate organic carbon in WG1 experiment for samples taken on Day 6. Horizontal line indicates the Day 0 value. See Table 1 for treatment abbreviations

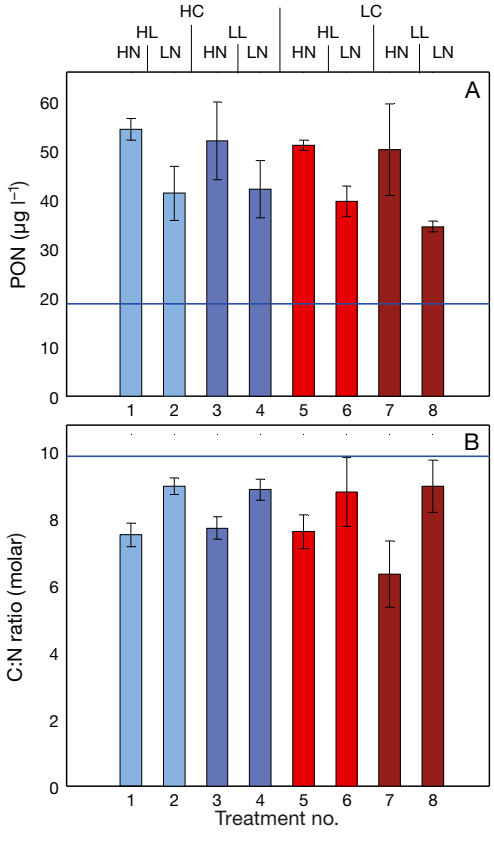

Fig. 5. Measurements of (A) particulate organic nitrogen and (B) the elemental ratio of particulate organic carbon to nitrogen (mol:mol) in WG1 experiment for samples taken on Day 6. Horizontal line indicates the Day 0 value

AAP bacteria abundance

Based on the heights of emission bands of bchl *a* and chl *a*, the aerobic anoxygenic bacteria formed 1.1 to 3.4% of the oxygenic phototrophs (data not shown). Although the heights of the emission bands are not a strictly quantitative measure of biomass, the estimated fraction of bchl *a*:chl *a* is well in line with recent estimates for relative AAP abundances in the Mediterranean based on absolute pigment measurements (Hojerová et al. 2011). The observed bchl *a*:chl *a* ratio was the highest on Day 6 (average 2.6%, compared to 1.5 and 1.6% on Days 2 and 4, respectively), indicating that AAP bacteria were thriving better than the oxygenic phytoplankton in the microcosms at the end of the experiment. There was also a significant correlation between the estimated AAP abundance from the emission band at 885 nm and the total heterotrophic bacterial counts (Spearman's rank order correlation, $p = 0.010$), indicating that the photoheterotrophic AAP bacteria formed a stable fraction of the heterotrophic bacterial community.

Phytoplankton abundance

The initial abundance of phytoplankton was consistent with mesotrophic coastal waters with an initial chl *a* concentration of ca. 0.85 µg l^{-1}. There was a steady increase in phytoplankton abundance from this initial level in all treatments with the most rapid growth and highest chl *a* level occurring in the HN treatments (Fig. 3G). Phytoplankton also increased in the LN treatments, an indication that nutrient enrichment was not the only factor favoring more growth. In the context of this overall growth trend, dramatic shifts occurred in the taxonomic composition of the assemblage over the course of the experiment. Initially, phytoplankton biomass was dominated by pico- and nanoplankton (<20 µm diameter) (Fig. 3H). Several species of diatoms were present in the initial sample and continued through the experiment, including *Leptocylindrus danicus, Chaetoceros* sp., *Guinardia striata, Nitzschia longissima*, and *Pseudonitzschia* sp. Effects of pre-screening through the 200 µm mesh were not evident on the initial diatom community composition. For instance, abundances of total diatoms and *Leptocylindrus danicus* in non-filtered samples were 205.5 and 103.6 cells ml^{-1}, respectively, compared to 218.8 and 115.5 cells ml^{-1} in pre-screened samples (Day 0). Furthermore, abundances of *Rhizosolenia* sp. and other large diatoms were lower than 5 cells ml^{-1} in both pre-filtered and filtered samples (for more details on taxonomic composition see Reul et al. 2014). Picophytoplankton increased over the first 2 d, most notably in the HN treatments, but declined several-fold between Days 2 and 4 (Fig. 3J; note log scale). Meanwhile, netplankton chl *a* (>20 µm diameter) increased to around 80% of chl *a* biomass by Day 4. This coincided with increased abundance of diatoms, the growth of which was already increasing on Day 2 and peaked on Day 4 (Fig. 3I). Subsequently, diatom biomass declined, coinciding with the depletion of silicate (Fig. 3C), and the netplankton fraction declined. Here, the response differed somewhat between HL and LL treatments; under HL, the percentage of chl *a* in the >20 µm fraction dropped to around 50% and there was some resurgence of the picophytoplankton. In LL, the netplankton percentage did not decrease as much and there was less recovery of the picophytoplankton. Overall, picophytoplankton increased significantly from Day 4 to Day 6 (Mann-Whitney *U*-test, $p = 0.008$). The LL response of diatoms differed between HC and LC (Fig. 3I). The highest biomass occurred under the HC HN LL treatment; the lowest under LC LN LL.

Treatment effects

Table 3 summarizes ANOVAs for the statistical significance of treatment effects on each response variable, considering responses over the entire experiment. Nutrient enrichment had the strongest effect on elemental composition and organism abundance in the experiment: responses are significant for N either as a direct effect over the whole experiment and/or as an interaction with time (repeated measures analysis) for all variables except CDOM (a_{250}). The probability of the *F*-ratio (p) was < 0.05 for POC and < 0.001 for other direct effects or interactions with time. CO_2 enrichment had a significant effect on DOC, otherwise CO_2 enrichment and irradiance had minor effects on elemental composition. On the other hand, these treatments had significant effects with time on phytoplankton abundance and composition. Interaction terms were generally not significant, except for the CO_2 × Irradiance interaction for chl *a*. This is related to the higher overall increase in chl *a* under LL for HC compared to LC, whereas the opposite was true for HL (i.e. there was less of an increase in chl *a* for HC compared to LC). All variables that were sampled with time had significant ($p < 0.05$ or 0.001, repeated measures ANOVA) interactions of at

Table 3. Microcosm experiment ANOVA results. *F*-ratios are shown for each treatment (C = CO_2, N = nutrients, L = irradiance; 2 levels each) and interactions. Particulate organic carbon (POC) and nitrogen (PON) and dissolved organic carbon (DOC) were sampled on Day 6; ANOVA is for main effects only. For other variables that were sampled several times (see Table 2 for frequency), results are for repeated measures ANOVAs for main effects, time and interaction terms. The 3-way interactions for main effects (C × N × L) were not significant for any variable. The 2-way interactions with time were not significant except for chl *a*: Time × C × L had an *F*-value of 4.69*. Abundance data (bacteria, picophytoplankton and chl *a*) was log transformed. Fract chl *a* > 20 µm: fraction of chl *a* in phytoplankton larger than 20 µm. *p < 0.05, **p < 0.01

	POC	PON	DOC	a_{250}	Bacteria	Picophytoplankton	Total chl *a*	Fract chl *a* > 20 µm
C	1.83	2.2	6.45*	1.95	0.43	0.05	0.02	0
N	4.79*	30.04**	0.04	4.12	15.05**	0	98.21**	0.72
L	0.42	0.81	0.31	3.51	2.38	3.77	0.77	1.08
C × N	0.31	0.25	1.76	6.31*	1.31	0.14	0.54	0.66
N × L	0.05	0	0.87	6.13*	0.17	0.11	2.49	0.37
C × L	0.4	0.29	0.91	3.25	0.18	0.65	4.57*	4.36
Time				106.0**	200.0**	631.0**	536.0**	89.44**
Time × C				10.12**	0.5	0.57	3.11*	2.18
Time × N				0.9	23.01**	28.73**	11.3**	4.34
Time × L				2.27	1.31	2.73	5.69**	12.86**

least one treatment effect with time, and there was also a significant Time × CO_2 × Irradiance interaction for total chl *a*. This shows that responses to treatments varied as the experiment progressed through a series of stages or phases. These phases are described in more detail in the 'Discussion'.

DISCUSSION

The results presented here provide a broad overview of how plankton (<200 µm) from the coastal Alboran Sea responds to the interactive manipulation of nutrients, CO_2 supply, and irradiance. Through the design of the experiment, there was another overriding manipulation of the community, which was the exclusion of 'larger' (meso- and macro-sized) zooplankton, and thus relaxation of grazing pressure on microplankton (both phytoplankton and microzooplankton). This initiated a series of quasi-successional events (trophic cascade) that can be summarized in 3 phases. These phases are discussed below and developed and explored in more detail in Mercado et al. (2014), Reul et al. (2014), and Sobrino et al. (2014). The phases are described in terms of the 3 intensive sampling times on Days 2, 4, and 6 since these present the most complete picture of the microcosm response. However, the smaller set of variables that were sampled daily, e.g. chl *a*, showed that the peak of each phase did not always happen on one of those days (see Mercado et al. 2014, Reul et al. 2014, Sobrino et al. 2014):

Phase 1 comprised Day 0 to Day 2 of the experiment, in which there was a general increase in biomass and abundance in all size categories and in all treatments, with a stronger increase in HN treatments (Fig. 3G–J). Detailed size distribution analysis showed that most of the increase occurred in the >6 µm size range, which would be associated with the growth of diatoms that experienced a relief from grazing pressure (Reul et al. 2014). Growth may have also been stimulated by relief from high-irradiance stress that the phytoplankton assemblage was experiencing due to near-surface stratification at the sampling station. The proportion of incident irradiance exposure was reduced from about 85% at the sampling station to 61% (HL) and 32% (LL). The initial increase in chl *a* was comparable to the difference between the surface and 5 m at the sampling station (cf. Figs. 1C & 3G). Reduced irradiance stress was also observed to increase extracellular release of organic carbon (EOC) from phytoplankton, a transient response associated with rebalancing carbon metabolism after changes in the irradiance environment (Sobrino et al. 2014). This may account for the peak in CDOM (a_{250}) during this period. In the HN treatments, there was a substantial increase in bacterial abundance which was enhanced by addition of organics+P as well as EOC, and the increase in small (pico/nano) plankton. There was apparently a very rapid sequestration of added phosphate by bacteria as it decreased to near initial levels even the first day after addition (data not shown), whereas there was little decrease in nitrate or increase in chl *a*.

Phase 2 comprised Days 2 to 4. This was the period of most dramatic changes in trophic structure. Bacteria and picophytoplankton assemblages were decimated, dropping to below initial levels. This was

apparently not due to nutrient exhaustion as more phosphate was added on Day 2 after P was found to be depleted. This leads to the conclusion that there must have been a secondary bloom of microzooplankton grazers that rapidly consumed small cells. Although microzooplankton were not a major focus of this study, there is evidence that ciliates increased at this time (Reul et al. 2014). At the same time, diatom growth accelerated, dominated by species too large to be affected by microzooplankton grazing (Reul et al. 2014), and which were also released from grazing pressure by the exclusion of zooplankton >200 µm (meso- and macrozooplankton). The bloom was dominated by diatoms >20 µm ESD, such as *Leptocylindrus danicus and Chaetoceros* sp. (Reul et al. 2014). The accumulation of biomass in the microcosms was further enhanced by the limitation of cell loss due to settling that would have been an important factor for diatom growth in the sampled surface layer (discussed further in Reul et al. 2014). The spurt of diatom growth depleted most of the remaining silicate. CDOM returned to near initial levels for HC treatments, consistent with microbial uptake (and reduced slope ratio), but slope ratio and a_{250} remained elevated in LC treatments. High EOC production under PAR conditions also continued for LC treatments, but was lower in HC treatments. EOC production is explored in more detail in Sobrino et al. (2014).

Phase 3 comprised Days 4 to 6. During this period, diatom growth stalled due to low silicate availability, and in the HN HL treatments, significant loss of cells occurred. Picophytoplankton and other non-diatom phytoplankton species resumed some growth, suggesting that microzooplankton may have decreased. The dominant phytoplankton cell size shifted back to smaller cells (Reul et al. 2014). Consistent with the latter was an increase in phytoplankton *in vivo* absorbance (normalized to chl *a*), from Day 4 to Day 6 (data not shown). In general, smaller cells are more efficient at absorbing PAR due to less shelf shading (Morel & Bricaud 1986). Bacterial growth resumed, which could have been fueled by excretion from silicate-starved diatoms or detritus produced by nonviable cells (see Sobrino et al. 2014).

Both HN and LN treatments followed the same general trends as described above, with the responses being more marked with nutrient enrichment. Bacterial and phytoplankton biomass were higher, and diatom and picophytoplankton abundance greater, in microcosms with added nutrients. POC and PON were also significantly enhanced, but nutrients did not significantly affect DOC and CDOM (a_{250}) (Table 3). The overall response to nutrients was consistent with the responses of a Mediterranean phytoplankton community in a previous mesocosm experiment with various levels of nutrient loading (Duarte et al. 2000). Diatoms were also the primary contributors to increased biomass in this previous experiment. In the present experiment, measures of phytoplankton abundance at ambient CO_2 were also higher at HL, indicating that this treatment level was not inhibiting to the studied assemblage. In contrast, bacterial abundance was not significantly different between high and low irradiance, suggesting phytoplankton and bacterioplankton were not tightly coupled. The relationship between autotrophic and heterotrophic plankton considering both biomass and production is examined in more detail by Mercado et al. (2014). CO_2 enrichment mainly had significant effects on the carbon-associated variables DOC and CDOM (a_{250}). However, these 2 variables (usually related) behaved differently; DOC was enhanced at HC while a_{250} was lower. The variation in rates of phytoplankton DOC release as measured in separate incubations (Sobrino et al. 2014) was more consistent with a_{250}, so the source of the additional DOC at HC is presently unknown.

A primary objective of the experiment was to test for interactions between treatment effects, each representing variables that are concurrently changing due to anthropogenic effects on the ocean. For the biological responses presented in this paper, which mainly represent state variables, there were few significant interactions. In particular, nutrients generally had an across-the-board effect, irrespective of CO_2 supply or irradiance. Similar results have been found in previous experiments crossing nutrient treatments with temperature or CO_2 (Song et al. 2014). There was a significant interaction for CO_2 supply and irradiance on total chl *a*. Under HC, chl *a* was inversely related to irradiance, whereas chl *a* was about the same in HL and LL under LC. This is consistent with the general observation that CO_2 enrichment increases performance at low light, but enhances sensitivity to inhibition at HL (Sobrino et al. 2008, 2009, Gao et al. 2012, Li et al. 2012). Indeed, photosynthetic rates (POC incorporation) under midday exposure conditions (UVR + PAR) were generally lower under HC than LC (Sobrino et al. 2014) when cells were acclimated to the high CO_2 conditions. Diatom abundance in HC was also less under HL vs. LL, but the statistical significance of the pattern could not be tested because diatoms were enumerated for only 1 of the 3 replicate microcosms. Interactions might be more important for certain assemblages

(e.g. calcifying microbes; Lefebvre et al. 2012), or for more extreme environmental variations (e.g. higher irradiance and UV exposure than occurred in this experiment). Significant treatment interactions were observed for the balance between production and respiration, as well as carbon and nitrogen uptake. Details are presented in Mercado et al. (2014).

In summary for this experiment, ecological control shifted from initially bottom-up to top-down, and back to bottom-up control over a 6 d period. The rapid pace of these shifts suggests that regulation of plankton assemblages in the Alboran sea can be very heterogeneous in space and time, consistent with previous field studies (Morán & Estrada 2001, Arin et al. 2002).

Acknowledgements. The experiments were performed in the framework of the workshop GAP9 that was partially financed by the University of Málaga (Program 'Plan Propio'). We are extensively grateful for the logistic and technical support from the Centro Oceanográfico de Málaga (Instituto Español de Oceanografía). P.N.'s contribution was supported by NASA grant NNX09AM85G. O.P. was supported by project Algatech (CZ.1.05/2.1.00/03.01100).

LITERATURE CITED

Arin L, Morán XAG, Estrada M (2002) Phytoplankton size distribution and growth rates in the Alboran Sea (SW Mediterranean): short term variability related to mesoscale hydrodynamics. J Plankton Res 24:1019–1033

Beardall J, Sobrino C, Stojkovic S (2009) Interactions between the impacts of ultraviolet radiation, elevated CO_2, and nutrient limitation on marine primary producers. Photochem Photobiol Sci 8:1257–1265

Bouvy M, Bettarel Y, Bouvier C, Domaizon I and others (2011) Trophic interactions between viruses, bacteria and nanoflagellates under various nutrient conditions and simulated climate change. Environ Microbiol 13:1842–1857

Boyd PW, Doney SC (2002) Modelling regional responses by marine pelagic ecosystems to global climate change. Geophys Res Lett 29:53-1–53-4

Boyd PW, Hutchins DA (2012) Understanding the responses of ocean biota to a complex matrix of cumulative anthropogenic change. Mar Ecol Prog Ser 470:125–135

Calbet A, Martínez RA, Isari S, Zervoudaki S and others (2012) Effects of light availability on mixotrophy and microzooplankton grazing in an oligotrophic plankton food web: evidences from a mesocosm study in Eastern Mediterranean waters. J Exp Mar Biol Ecol 424–425: 66–77

Caldeira K, Wickett ME (2003) Oceanography: anthropogenic carbon and ocean pH. Nature 425:365

Caron DA, Hutchins DA (2013) The effects of changing climate on microzooplankton grazing and community structure: drivers, predictions and knowledge gaps. J Plankton Res 35:235–252

CIESM (2008) Impacts of acidification on biological, chemical and physical systems in the Mediterranean and Black Seas. CIESM Monograph No. 36, Monaco

Doney SC, Ruckelshaus M, Duffy JE, Barry JP and others (2012) Climate change impacts on marine ecosystems. Annu Rev Mar Sci 4:11–37

Duarte CM, Agusti S, Agawin NSR (2000) Response of a Mediterranean phytoplankton community to increased nutrient inputs: a mesocosm experiment. Mar Ecol Prog Ser 195:61–70

Feely RA, Orr J, Fabry VJ, Kleypas JA, Sabine CL, Langdon C (2009) Present and future changes in seawater chemistry due to ocean acidification. AGU Geophys Monogr Ser 183:175–188

Folt CL, Chen CY, Moore MV, Burnaford J (1999) Synergism and antagonism among multiple stressors. Limnol Oceanogr 44:864–877

Gao K, Helbling EW, Häder DP, Hutchins DA (2012) Responses of marine primary producers to interactions between ocean acidification, solar radiation, and warming. Mar Ecol Prog Ser 470:167–189

Gargett AE, Marra J (2002) Effects of upper ocean physical processes (turbulence, advection, and air-sea interaction) on oceanic primary production. In: Robinson AR, McCarthy JJ, Rothschild BJ (eds) The sea, Vol 12. Wiley, New York, NY, p 19–49

Grashoff K, Erhardt M, Kremling K (1983) Methods of seawater analysis. Wiley-VCH, Weinheim

Halpern BS, Walbridge S, Selkoe KA, Kappel CV and others (2008) A global map of human impact on marine ecosystems. Science 319:948–952

Helms JR, Stubbins A, Ritchie JD, Minor EC, Kieber DJ, Mopper K (2008) Absorption spectral slopes and slope ratios as indicators of molecular weight, source, and photobleaching of chromophoric dissolved organic matter. Limnol Oceanogr 53:955–969

Hojerová E, Mašín M, Brunet C, Ferrera I, Gasol JM, Koblížek M (2011) Distribution and growth of aerobic anoxygenic phototrophs in the Mediterranean Sea. Environ Microbiol 13:2717–2725

Huertas IE, Ríos AF, García-Lafuente J, Makaoui A and others (2009) Anthropogenic and natural CO_2 exchange through the Strait of Gibraltar. Biogeosciences 6:647–662

IPCC (2013) Climate change 2013: the physical science basis. In: Stocker TF, Qin D, Plattner GK, Tignor M and others (eds) Contribution of Working Group I to the Fifth Assessment Report of the Intergovernmental Panel on Climate Change. Cambridge University Press, Cambridge

Lefebvre SC, Benner I, Stillman JH, Parker AE and others (2012) Nitrogen source and pCO_2 synergistically affect carbon allocation, growth and morphology of the coccolithophore *Emiliania huxleyi*: potential implications of ocean acidification for the carbon cycle. Glob Change Biol 18:493–503

Li W, Gao K, Beardall J (2012) Interactive effects of ocean acidification and nitrogen-limitation on the diatom *Phaeodactylum tricornutum.* PLoS ONE 7:e51590

Litchman E, Edwards KF, Klausmeier CA, Thomas MK (2012) Phytoplankton niches, traits and eco-evolutionary responses to global environmental change. Mar Ecol Prog Ser 470:235–248

MacIsaac EA, Stockner JG (1993) Enumeration of phototrophic picoplankton by autofluorescence microscopy. In: Kemp PF, Sherr BF, Sherr EB, Cole JJ (eds) Handbook of methods in aquatic microbial ecology. CRC Press, Boca Raton, FL, p 187–197

Marie D, Partensky F, Jacquet S, Vaulot D (1997) Enumeration and cell cycle analysis of natural populations of marine picoplankton by flow cytometry using the nucleic acid stain SYBR Green I. Appl Environ Microbiol 63: 186–193

Martínez-García S, Fernández E, Álvarez-Salgado X-A, González J and others (2010) Differential responses of phytoplankton and heterotrophic bacteria to organic and inorganic nutrient additions in coastal waters off the NW Iberian Peninsula. Mar Ecol Prog Ser 416:17–33

McKenzie RL, Aucamp PJ, Bais AF, Bjorn LO, Ilyas M, Madronich S (2011) Ozone depletion and climate change: impacts on UV radiation. Photochem Photobiol Sci 10: 182–198

Mercado JM, Cortés D, García A, Ramírez T (2007) Seasonal and inter-annual changes in the planktonic communities of the northwest Alboran Sea (Mediterranean Sea). Prog Oceanogr 74:273–293

Mercado JM, Cortés D, Ramírez T, Gómez F (2012) Hydrological forcing masks the potential impact of nutrient release from diffuse sources in the NW coast of the Alboran Sea. Hydrobiologia 680:91–107

Mercado JM, Sobrino C, Neale PJ, Segovia M and others (2014) Effect of CO_2, nutrients and light on coastal plankton. II. Metabolic rates. Aquat Biol 22:43–57

Morán XAG, Estrada M (2001) Short-term variability of photosynthetic parameters and particulate and dissolved primary production in the Alboran Sea (SW Mediterranean). Mar Ecol Prog Ser 212:53–67

Morel A, Bricaud A (1986) Inherent optical properties of algal cells including picoplankton: theoretical and experimental results. In: Platt T, Li WKW (eds) Photosynthetic picoplankton. Canadian Bull Fisheries Aquat Sci no. 214, Ottawa, p 521–559

Neale PJ, Bossard P, Huot Y, Sommaruga R (2001) Incident and *in situ* irradiance in Lakes Cadagno and Lucerne: a comparison of methods and models. Aquat Sci 63: 250–264

Neale PJ, Goodrich VR, Brinley WR (2005) The Smithsonian-NIST-USDA-FPL network for monitoring solar ultraviolet irradiance: comparison of radiometer measurements and radiative transfer model calculations. In: Martin JW, Ryntz RA, Dickie RA (eds) Service life prediction: challenging the status quo. Federation of Societies for Coatings Technology, Blue Bell, PA, p 159–170

Pegau WS, Gray D, Zaneveld JRV (1997) Absorption and attenuation of visible and near-infrared light in water: dependence on temperature and salinity. Appl Opt 36: 6035–6046

Porter KG, Feig YS (1980) The use of DAPI for identifying and counting aquatic microflora. Limnol Oceanogr 25: 243–248

Prášil O, Bína D, Medová H, Řeháková K, Zapomělová E, Veselá J, Oren A (2009) Emission spectroscopy and kinetic fluorometry studies of phototrophic microbial communities along a salinity gradient in solar saltern evaporation ponds of Eilat, Israel. Aquat Microb Ecol 56: 285–296

Rabalais NN, Turner RE, Díaz RJ, Justi D (2009) Global change and eutrophication of coastal waters. ICES J Mar Sci 66:1528–1537

Ramírez T, Cortés D, Mercado JM, Vargas-Yañez M, Sebastián M, Liger E (2005) Seasonal dynamics of inorganic nutrients and phytoplankton biomass in the NW Alboran Sea. Estuar Coast Shelf Sci 65:654–670

Reul A, Muñoz M, Bautista B, Neale PJ and others (2014) Effect of CO_2, nutrients and light on coastal plankton. III. Trophic cascade, size structure and composition. Aquat Biol 22:59–76

Riebesell U, Bellerby RGJ, Grossart HP, Thingstad F (2008) Mesocosm CO_2 perturbation studies: from organism to community level. Biogeosciences 5:1157–1164

Ros M, Miracle MR (1984) Seasonal distribution of the dinoflagellates in the Mar Menor (Murcia, Spain). Ann Biol 2: 169–180

Ruggaber A, Dlugi R, Nakajima T (1994) Modeling of radiation quantities and photolysis frequencies in the troposphere. J Atmos Chem 18:171–210

Schneider A, Wallace DWR, Körtzinger A (2007) Alkalinity of the Mediterranean Sea. Geophys Res Lett 34:L15608, doi:10.1029/2006GL028842

Sobrino C, Ward ML, Neale PJ (2008) Acclimation to elevated carbon dioxide and ultraviolet radiation in the diatom *Thalassiosira pseudonana*: effects on growth, photosynthesis, and spectral sensitivity of photoinhibition. Limnol Oceanogr 53:494–505

Sobrino C, Neale PJ, Phillips-Kress JD, Moeller RE, Porter JA (2009) Elevated CO_2 increases sensitivity to ultraviolet radiation in lacustrine phytoplankton assemblages. Limnol Oceanogr 54:2448–2459

Sobrino C, Segovia M, Neale PJ, Mercado JM and others (2014) Effect of CO_2, nutrients and light on coastal plankton. IV. Physiological responses Aquat Biol 22:77–93

Song C, Ballantyne F IV, Smith VH (2014) Enhanced dissolved organic carbon production in aquatic ecosystems in response to elevated atmospheric CO_2. Biogeochemistry 118:49–60

Thomas MK, Kremer CT, Klausmeier CA, Litchman E (2012) A global pattern of thermal adaptation in marine phytoplankton. Science 338:1085–1088

Tomas CR (1997) Identifying marine phytoplankton. Academic Press, London

Touratier F, Goyet C (2009) Decadal evolution of anthropogenic CO_2 in the northwestern Mediterranean Sea from the mid-1990s to the mid-2000s. Deep-Sea Res I 56: 1708–1716

Utermöhl H (1958) Zur Vervollkommnung der quantitativen Phytoplankton-Methodik. Mitt Int Ver Theor Angew Limnol 9:1–38

Vargas-Yáñez M, Ramírez T, Cortés D, Sebastián M, Plaza F (2002) Warming trends in the continental shelf of Málaga Bay (ALBORÁN SEA). Geophys Res Lett 29:39-1–39-4, doi:101029/2002/GL015306

Vidussi F, Mostajir B, Fouilland E, Floc'h EL and others (2011) Effects of experimental warming and increased ultraviolet B radiation on the Mediterranean plankton food web. Limnol Oceanogr 56:206–218

Vitousek PM, Mooney HA, Lubchenco J, Melillo JM (1997) Human domination of Earth's ecosystems. Science 277: 494–499

Weatherhead EC, Andersen SB (2006) The search for signs of recovery of the ozone layer. Nature 441:39–45

Winder M, Sommer U (2012) Phytoplankton response to a changing climate. Hydrobiologia 698:5–16

WMO (World Meteorological Organization) (2011) Scientific assessment of ozone depletion: 2010, Global Ozone Research and Monitoring Project–Report No. 52. WMO, Geneva www.wmo.int/pages/prog/arep/gaw/ozone/

Yentsch C, Menzel D (1963) A method for the determination of phytoplankton chlorophyll and phaeophytin by fluorescence. Deep-Sea Res 10:221–231

Zeebe RE, Wolf-Gladrow D (2001) Appendix C: details and calculations. In: Zebee RE, Wolf-Gladrow D (eds) CO_2 in seawater: equilibrium, kinetics, isotopes. Elsevier, Amsterdam, p 279–304

Appendix. Measurements of the partial pressure of CO_2 (pCO_2) and dissolved inorganic carbon (DIC) in the GAP WG1 microcosm experiment. The mean ± SD of measurements of 3 replicate microcosms are tabulated for each of 8 different treatment combinations with a high and low level of CO_2 enrichment (HC, LC), nutrient addition (HN, LN), and irradiance (HL, LL) (see 'Materials and methods' for details). Measurements were made daily, except on Day 5. The initial (Day 0) values were pCO_2 511.3 ± 10.4 µatm, DIC 2459.2 ± 120.4 µmol l^{-1}

Treat. no.	CO_2 supply	Nutrients	Solar irradiance	pCO_2 (µatm) Day 1	Day 2	Day 3	Day 4	Day 6
1	HC	HN	HL	736.7 ± 55.0	1033.9 ± 37.4	1278.7 ± 271.2	1977.5 ± 153.3	1219.5 ± 59.2
2	HC	LN	HL	671.8 ± 128.3	925.2 ± 155.0	1003.4 ± 158.6	1666.9 ± 434.5	1143.9 ± 76.0
3	HC	HN	LL	755.6 ± 26.6	1014.6 ± 68.6	1050.2 ± 30.3	904.6 ± 22.9	881.0 ± 49.3
4	HC	LN	LL	696.9 ± 46.0	1042.0 ± 37.2	1019.5 ± 15.2	912.0 ± 27.0	1066.1 ± 56.7
5	LC	HN	HL	499.7 ± 33.8	509.4 ± 25.0	526.9 ± 19.9	409.6 ± 13.0	352.7 ± 81.1
6	LC	LN	HL	445.9 ± 11.0	528.4 ± 24.8	475.2 ± 24.9	397.7 ± 12.9	407.1 ± 9.0
7	LC	HN	LL	480.7 ± 9.5	521.5 ± 12.0	468.2 ± 19.7	412.0 ± 31.9	400.9 ± 6.2
8	LC	LN	LL	445.2 ± 3.5	501.4 ± 32.1	445.9 ± 16.4	411.5 ± 9.3	426.6 ± 12.1
				DIC (µmol l^{-1}) Day 1	Day 2	Day 3	Day 4	Day 6
1	HC	HN	HL	2400.6 ± 81.2	2671.3 ± 67.9	2728.6 ± 198.4	2509.2 ± 49.8	2655.4 ± 11.6
2	HC	LN	HL	2355.7 ± 106.3	2633.2 ± 74.4	2609.4 ± 157.6	2263.7 ± 62.1	2533.2 ± 147.0
3	HC	HN	LL	2534.0 ± 84.5	2668.8 ± 47.5	2530.4 ± 75.6	2186.1 ± 57.7	2355.8 ± 7.5
4	HC	LN	LL	2393.9 ± 95.4	2682.6 ± 76.9	2478.0 ± 56.2	2205.1 ± 51.8	2571.6 ± 76.1
5	LC	HN	HL	2442.6 ± 111.0	2449.1 ± 46.4	2566.6 ± 30.6	2090.9 ± 65.7	2181.7 ± 37.3
6	LC	LN	HL	2273.5 ± 21.0	2561.2 ± 38.8	2356.8 ± 161.2	2028.3 ± 36.1	2256.5 ± 55.0
7	LC	HN	LL	2348.3 ± 50.6	2569.4 ± 103.7	2348.9 ± 107.8	2096.6 ± 108.2	2234.5 ± 40.2
8	LC	LN	LL	2286.9 ± 20.0	2597.6 ± 188.5	2292.7 ± 22.3	2150.4 ± 25.3	2299.3 ± 71.7

Submitted: December 18, 2013; Accepted: June 25, 2014 *Proofs received from author(s): October 13, 2014*